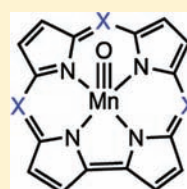


Low-Energy States of Manganese–Oxo Corrole and Corrolazine: Multiconfiguration Reference *ab Initio* CalculationsHailiang Zhao,[†] Kristine Pierloot,^{*,†} Ernie H. G. Langner,[‡] Jannie C. Swarts,[‡] Jeanet Conradie,^{‡,§} and Abhik Ghosh^{*,§}[†]Department of Chemistry, University of Leuven, Celestijnenlaan 200F, B-3001 Heverlee-Leuven, Belgium[‡]Department of Chemistry, University of the Free State, 9300 Bloemfontein, Republic of South Africa[§]Department of Chemistry and Center for Theoretical and Computational Chemistry, University of Tromsø, 9037 Tromsø, Norway

Supporting Information

ABSTRACT: Manganese(V)–oxo corrole and corrolazine have been studied with *ab initio* multiconfiguration reference methods (CASPT2 and RASPT2) and large atomic natural orbital (ANO) basis sets. The calculations confirm the expected singlet d_5^2 ground states for both complexes and rule out excited states within 0.5 eV of the ground states. The lowest excited states are a pair of Mn(V) triplet states with $d_5^1 d_{\pi}^1$ configurations 0.5–0.75 eV above the ground state. Manganese(IV)–oxo macrocycle radical states are much higher in energy, ≥ 1.0 eV relative to the ground state. The macrocyclic ligands in the ground states of the complexes are thus unambiguously ‘innocent’. The approximate similarity of the spin state energetics of the corrole and corrolazine complexes suggests that the latter macrocycle on its own does not afford any special stabilization for the Mn^VO center. The remarkable stability of an Mn^VO octaarylcorrolazine thus appears to be ascribable to the steric protection afforded by the β -aryl groups.



Mn(Cor)(O): X = CH
Mn(Cz)(O): X = N

INTRODUCTION

Well known for some time,¹ Mn^VO intermediates based on porphyrin-type ligands are of considerable interest on account of their ability to catalyze oxo atom transfer (OAT) reactions.^{2–4} As diamagnetic d_5^2 species, they are less reactive than their Mn^{IV}O⁵ and Fe^{IV}O⁶ counterparts with half-occupied antibonding d_{π} – p_{π} MOs. Their stability varies considerably with the equatorial ligand. Although a nonporphyrinoid complex based on a macrocyclic tetraamido-*N* ligand remains a rare example of a crystallographically characterized Mn^VO complex,⁷ a number of Mn^VO corrole and corrolazine derivatives have been isolated as solid, pure compounds.^{2–4} While the Mn^VO corroles vary in stability,^{2–4} Goldberg et al. reported an unusually stable Mn^VO β -octaarylcorrolazine derivative, which, though not yet crystallographically characterized, is stable enough to be chromatographed at room temperature.⁸ In light of our earlier work on corrole chemistry, where ligand noninnocence is ubiquitous,⁹ these observations raise the following questions: (1) How much higher in energy, relative to the d_5^2 Mn^VO ground states, are the Mn^{IV}O corrole radical states? (2) Is the stability of the Mn^VO octaarylcorrolazine largely electronic in origin or do steric effects play a major role?⁸ Unfortunately, one of the known limitations of DFT is in the area of transition metal spin state energetics;^{10–12} the problem is particularly acute for oxidized heme species, where DFT often indicates a high-valent iron center, whereas experiments indicate a porphyrin radical formulation.^{10,13,14} An instructive example of this issue is provided by charge-neutral difluoroiron porphyrin species, for which DFT methods suggested an Fe(IV) description whereas *ab initio* CASPT2

calculations indicated an Fe^{III}(Por^{•-})F₂ formulation.¹⁵ Very recently, NMR studies have confirmed the radical formulation indicated by CASPT2.¹⁶ Even for Mn^VO porphyrins, DFT behaves somewhat erratically, with certain B3LYP calculations predicting a triplet ground state, contrary to experimental observations.¹⁷ Benchmarking the excited state energetics of Mn^VO porphyrinoids against high-level *ab initio* methods is thus of considerable importance. Herein, we used DFT and multiconfigurational *ab initio* methods to study the low-energy states of Mn(Cor)(O) and Mn(Cz)(O) (depicted below), where Cor³⁻ and Cz³⁻ are the trianions of corrole and corrolazine, respectively.



Mn(Cor)(O): X = CH
Mn(Cz)(O): X = N

COMPUTATIONAL METHODS

Full DFT geometry optimizations were performed with three functionals, BP86,^{18,19} PBE0,²⁰ and B3LYP(VWN III),²¹ as implemented in the Turbomole 6.0 program package.²² Single-point calculations with the OLYP functional²³ were carried out on PBE0-optimized structures with the Gaussian03 program.²⁴ All optimizations were performed within the *C_s* symmetry group, and in all reported

Received: September 10, 2011

Published: March 20, 2012

Table 1. Relative Energy (eV) of the Lowest Lying Electronic States of MnO(Cor) with Respect to the $1^1A'$ Ground State^a

state	configuration	BP86	B3LYP	PBE0	OLYP	BSI		BSII	
						CASPT2	RASPT2	CASPT2	RASPT2
Mn(V)O(Cor ³⁻)									
$1^1A'$	$(d_{x^2-y^2})^2$	0.00	0.00	0.00	0.00	0.00	0.00	0.00	0.00
$1^3A'$	$(d_{x^2-y^2})^1(d_{xz})^1$	0.74	0.52	0.34	0.66	0.41	0.32	0.53	0.36
$1^3A''$	$(d_{x^2-y^2})^1(d_{yz})^1$	0.78	0.53	0.35	0.71	0.51	0.38	0.63	0.41
Mn(IV)O(Cor ^{•2-}) (“ a_{2u} ”) ¹									
$1^5A''$	$(d_{x^2-y^2})^1(d_{xz})^1(d_{yz})^1(a'')^1$	1.29	0.49	0.33	1.03	0.80	0.81	1.00	1.02
$2^3A'$	$(d_{x^2-y^2})^2(d_{xz})^1(a')^1$	NP ^b	0.47	0.44	NP ^b	0.93	0.90	1.11	1.08
$2^3A''$	$(d_{x^2-y^2})^2(d_{yz})^1(a'')^1$	NP ^b	0.49	0.45	NP ^b	0.95	0.92	1.13	1.10
Mn(IV)O(Cor ^{•2-}) (“ a_{1u} ”) ¹									
$1^5A'$	$(d_{x^2-y^2})^1(d_{xz})^1(d_{yz})^1(a'')^1$	1.39	0.60	0.46	1.16	1.28	1.05	1.50	1.26
$3^3A''$	$(d_{x^2-y^2})^2(d_{xz})^1(a'')^1$	1.13	0.55	0.54	1.06	1.37	1.11	1.56	1.29
$3^3A'$	$(d_{x^2-y^2})^2(d_{yz})^1(a'')^1$	1.15	0.57	0.56	1.08	1.46	1.14	1.63	1.32

^aThe occupation of the main configuration is indicated for each state. The a' - and a'' -type orbitals are the corrole π HOMOs. C_s symmetry with the xz plane as the symmetry plane. ^bNP = These calculations were not possible because of a lower lying state of the same spin/symmetry.

Table 2. Relative Energy (eV) of the Lowest Lying Electronic States of MnO(Cz) with Respect to the $1^1A'$ State^a

state	configuration	BP86	B3LYP	PBE0	OLYP	BSI		BSII	
						CASPT2	RASPT2	CASPT2	RASPT2
Mn(V)O(Cz ³⁻)									
$1^1A'$	$(d_{x^2-y^2})^2$	0.00	0.00	0.00	0.00	0.00	0.00	0.00	0.00
$1^3A'$	$(d_{x^2-y^2})^1(d_{xz})^1$	0.82	0.68	0.57	0.71	0.51	0.44	0.55	0.50
$1^3A''$	$(d_{x^2-y^2})^1(d_{yz})^1$	0.86	0.69	0.58	0.75	0.64	0.49	0.69	0.53
Mn(IV)O(Cz ^{•2-}) (“ a_{1u} ”) ¹									
$2^3A''$	$(d_{x^2-y^2})^2(d_{xz})^1(a'')^1$	1.23	0.66	0.66	1.18	1.62	1.21	1.77	1.34
$2^3A'$	$(d_{x^2-y^2})^2(d_{yz})^1(a'')^1$	1.25	0.71	0.71	1.22	1.63	1.25	1.77	1.40
$1^5A'$	$(d_{x^2-y^2})^1(d_{xz})^1(d_{yz})^1(a'')^1$	1.66	0.87	0.75	1.46	1.64	1.29	1.82	1.46
Mn(IV)O(Cz ^{•2-}) (“ a_{2u} ”) ¹									
$1^5A''$	$(d_{x^2-y^2})^1(d_{xz})^1(d_{yz})^1(a'')^1$	2.08	1.41	1.31	1.87	1.84	1.78	2.00	1.95
$3^3A'$	$(d_{x^2-y^2})^2(d_{xz})^1(a'')^1$	NP ^b	1.24	1.26	1.46	1.86	1.72	1.98	1.95
$3^3A''$	$(d_{x^2-y^2})^2(d_{yz})^1(a'')^1$	NP ^b	NP ^b	NP ^{b,c}	NP ^b	1.91	1.77	2.04	2.01

^aThe occupation of the main configuration is indicated for each state. The a' - and a'' -type orbitals are the corrolazine π HOMOs. C_s symmetry with the xz plane as the symmetry plane. ^bNP = These calculations were not possible because of a lower lying state of the same spin/symmetry. ^cFor this state, CASPT2/RASPT2 calculations were performed at the corresponding $^3A'$ geometry.

results the structures are placed such that the symmetry plane corresponds to the xz plane. Accordingly, the manganese 3d orbitals d_{z^2} , d_{xz} , and $d_{x^2-y^2}$ are symmetric (a') with respect to this plane, while d_{yz} and d_{xy} are antisymmetric (a''). Also note that the coordinating N are situated in between the x and the y axes, such that the Mn d_{xy} orbital is involved in σ bonding, while the $d_{x^2-y^2}$ orbital is essentially nonbonding. All DFT calculations were performed with def2-TZVP basis sets.²⁵ The spin-unrestricted formalism was used in all cases. For the closed-shell Mn(V) $1^1A'$ ground state, a restricted solution ($\langle S^2 \rangle = 0.0$) was obtained.

CASPT2²⁶ and RASPT2²⁷ calculations were performed with Molcas 7.4²⁸ using a scalar-relativistic second-order Douglas–Kroll Hamiltonian,²⁹ the standard IPEA-shifted zero-order Hamiltonian for second-order perturbation theory,³⁰ and Cholesky decomposition of the two-electron repulsion integrals³¹ (the decomposition threshold was set to 10^{-6} au). Single-point calculations were performed on top of the PBE0 structures obtained for each electronic state. Two combinations of ANO-type basis sets were used for the CASPT2/RASPT2 calculations: Basis I consists of the following: Mn ANO-*rcc*³² contracted to [7s6p5d2f1g]; N, C, O ANO-*s*³³ contracted to [4s3p1d]; H ANO-*s* contracted to [2s]. Basis II combines ANO-*rcc* basis sets on all atoms, contracted to [7s6p5d3f2g1h] for Mn, [4s3p2d1f] for N, C, O, and [3s1p] for H. In all CASPT2 and RASPT2 calculations only the valence electrons, including Mn(3s,3p), were correlated.

The CASPT2 calculations were based on a CAS(14,16) wave function, constructed according to the standard rules for transition

metal compounds.^{34–36} Nondynamical correlation effects involving the Mn 3d electrons, the Mn–O bond, and the Mn–C σ bond (C = Cor, Cz), are described by making active four pairs of bonding–antibonding orbitals (Mn3d_{z²}–O2p_z), (Mn3d_{xz}–O2p_x), (Mn3d_{yz}–O2p_y), (Mn3d_{xy}–C σ_{xy}), the remaining nonbonding Mn 3d_{x²–y²} orbital, and three double-shell orbitals (4d_{x²–y²}, mixed 4d_{xz}–O3p_x, mixed 4d_{yz}–O3p_y). To allow electron transitions between the Mn and C fragments, the ‘Gouterman’ set of two HOMO C π orbitals (“ a_{1u} ” a_{2u} ”) and their correlating LUMO π^* orbitals (“ e_g ”) were also made active. Plots of the active orbitals of the CASSCF calculations are provided in Figures S1 (Mn(Cor)(O)) and S2 (Mn(Cz)(O)), Supporting Information.

The RASPT2 calculations were based on a global RAS(28,27) active space, obtained by extending the CAS(14,16) space with a selection of C (π , π^*) orbitals (that is, excluding only the four C (π , π^*) couples located on the corrole β -carbons). In a RASSCF calculation the global active space is further subdivided into three subspaces (RAS1, RAS2, RAS3).²⁷ For each state, the orbitals in RAS2 were kept limited to the three couples of bonding–antibonding Mn3d–O2p orbitals and all (remaining) singly occupied orbitals. Up to double excitations were allowed out of RAS1 and into RAS3. Plots of the active orbitals of the RASSCF calculations are provided in Figures S3 (Mn(Cor)(O)) and S4 (Mn(Cz)(O)), Supporting Information. Detailed descriptions and benchmarking of the RASPT2 method for heme systems have been reported in the literature.^{37,38} The CASPT2/RASPT2 relative energetics are believed to be accurate to 0.1–0.2 eV.

RESULTS AND DISCUSSION

All four exchange-correlation functionals reproduce the very short Mn–O distances observed experimentally (~ 1.52 Å) as well as the short equatorial Mn–N distances (~ 1.92 Å for Cor and 1.90 Å for Cz; see Table S1, Supporting Information, for details). Geometries optimized with PBE0 and the def2-TZVP basis set were used in the single-point ab initio calculations. Tables 1 and 2 present our results on the spin state energetics of the two complexes studied. All methods examined reproduce the observed singlet ground state with a $d_{x^2-y^2}^2 (d_\delta^2)$ Mn(V) center (recall that the $d_{x^2-y^2}$ orbital, in our notation, is the in-plane nonbonding d orbital).³⁹ Some of the more interesting conclusions to emerge from the data are as follows.

For both complexes, the lowest excited states correspond to a pair of d–d-excited triplet Mn(V) states $d_{x^2-y^2}^1 d_{xz}^1$ and $d_{x^2-y^2}^1 d_{yz}^1$ configurations (see, however, the Supporting Information for more details concerning the nature of these states with different methods). Understandably, in light of the localized nature of the excitations, all methods, both DFT and ab initio, yield relatively consistent energies for these states: ~ 0.5 – 0.75 eV above the ground state; the classic pure functional BP86 gives a slightly higher energy of 0.86 eV, but this is not unexpected.

The energies of Mn^{IV}O–(Cor/Cz)^{•2-} radical states vary more, both between the two complexes studied and as a function of the computational method chosen. Thus, for Mn(Cor)(O), the lowest quintet $1^5A'$ state, which has a $d_{x^2-y^2}^1 d_{xz}^1 d_{yz}^1 "a_{2u}"^1$ configuration (where we used the familiar porphyrin D_{4h} notation for the a' corrole HOMO), is found at about 0.8 – 1.0 eV with the ab initio methods and OLYP, slightly higher at about 1.2 eV with BP86 but drastically lower at <0.5 eV with the hybrid functionals PBE0 and B3LYP. The analogous Mn^{IV}O " a_{1u} " radical state is slightly higher in energy, at about 1.25 – 1.5 eV, according to the ab initio methods and the two pure functionals BP86 and OLYP; once again, the two hybrid functionals examined predict dramatically lower energies. Elsewhere, we encountered a number of additional examples where the OPTX-based pure functionals outperformed hybrid functionals with respect to the issue of spin state energetics.^{40–42}

The energies of the " a_{1u} " and " a_{2u} " radical states are reversed for Mn(Cz)(O), relative to Mn(Cor)(O); this is expected because meso-triazasubstitution is expected to stabilize the " a_{2u} " MO, which has large amplitudes at the meso positions. Thus, for Mn(Cz)(O), the lowest quintet state is an A' state with a $d_{x^2-y^2}^1 d_{xz}^1 d_{yz}^1 "a_{1u}"^1$ configuration. RASPT2 and the pure functionals indicate an energy of ~ 1.25 eV, whereas CASPT2 indicates a somewhat higher energy of ~ 1.6 – 1.7 eV, and the hybrid functionals, once again, predict a low energy of about 0.7 eV. The analogous Mn^{IV}O " a_{2u} " radical state is >1.5 eV with both the pure functionals and ab initio methods and somewhat lower with the hybrid functionals. Ab initio methods thus provide valuable calibration for DFT and indicate that hybrid functionals do not necessarily provide better spin state energetics than pure functionals.

The above results have a number of chemical implications. First, although ubiquitous in corrole chemistry,⁹ a noninnocent macrocycle is by no means universal. Even for high-valent iron, a strongly donating axial ligand such as aryl stabilizes a "true" Fe(IV) state. In the same vein, Cr^VO corroles are believed to contain an innocent macrocycle. By contrast, copper corroles are noninnocent and best described as Cu^{II}Cor^{•2-}. Copper

corroles are also unique in that their noninnocence drives a dramatic saddling of the macrocycle.⁴³ Silver⁴⁴ and gold^{45,46} corroles are relatively innocent by comparison. Against this context, both DFT and ab initio calculations indicate Mn^VO ground states for both corroles and corrolazines by an unambiguous margin of energy; Mn^{IV}O macrocycle radical states are an electronvolt or higher in energy for both corroles and corrolazines.⁴⁷

Second, to a first approximation, the energy ordering of states of different character are similar for both complexes studied

$$S = 0 \text{ Mn}^{\text{V}}\text{O} < S = 1 \text{ Mn}^{\text{V}}\text{O} \ll \text{Mn}^{\text{IV}}\text{O}-(\text{Cor/Cz})^{\bullet 2-}$$

In other words, the corrolazine macrocycle does not confer any special stability on the singlet ground state relative to corroles. Moreover, CASPT2 calculations (with basis set BSII) predict roughly similar adiabatic electron affinities for both complexes: 2.17 and 2.41 eV for Mn^VO Cor and Mn^VO Cz, respectively (where the reduced state is the $^4A'$, $(d_{x^2-y^2})^1(d_{xz})^1(d_{yz})^1$ anionic Mn(IV) state). The observed stability of the Mn^VO octaarylcorrolazine complex reported by Goldberg et al. thus seems attributable to steric protection afforded by the peripheral substituents. Indeed, based on electronic considerations alone, an Mn^VO corrolazine is expected to be more reactive than an analogous corrole on account of its greater electron-deficient character and higher electron affinity. Consistent with this picture is recent synthesis of relatively stable Mn^VO complexes with sterically hindered corrole ligands by Gross et al.^{4a}

In summary, ab initio and DFT calculations have shown that the strongly π -donating oxo ligand can stabilize a d_δ^2 Mn^VO ground state by an unambiguous margin of energy for both corroles and corrolazines. The lowest excited states are d–d-excited Mn^VO triplet states, some 0.5 eV above the ground states. By contrast, Mn^{IV}O macrocycle radical states are an electronvolt or higher in energy relative to the ground states. We have shown that, depending the functional, DFT performs rather erratically with respect to the energetics of the radical states. Multiconfigurational ab initio methods, by contrast, appear to provide a balanced and accurate description of all states examined.

ASSOCIATED CONTENT

Supporting Information

Key bond distances and Cartesian coordinates for all states obtained from PBE0; plots of the natural CAS(14,16) active orbitals and pseudonatural RAS(28,27) active orbitals and their occupation numbers; detailed information on the geometric and electronic structure (spin densities) for the three lowest states, as obtained with different DFT functionals and with CASSCF/RASSCF. This material is available free of charge via the Internet at <http://pubs.acs.org>.

AUTHOR INFORMATION

Corresponding Author

*E-mail: kristin.pierloot@chem.kuleuven.be (K.P.); abhik.ghosh@uit.no (A.G.).

Notes

The authors declare no competing financial interest.

ACKNOWLEDGMENTS

This work was supported by the Research Council of Norway, the Flemish Science Foundation (FWO), and the Concerted Research Action of the Flemish Government (GOA) and the National Research Fund of the Republic of South Africa.

REFERENCES

- (1) (a) Groves, J. T.; Kruper, W. J.; Haushalter, R. C. *J. Am. Chem. Soc.* **1980**, *102*, 6375–6377. (b) Jin, N.; Groves, J. T. *J. Am. Chem. Soc.* **1999**, *121*, 2923–2924. (c) Jin, N.; Bourassa, J. L.; Tizio, S. C.; Groves, J. T. *Angew. Chem., Int. Ed.* **2000**, *39*, 3849–3851.
- (2) Early reports of Mn^{VO} corroles: (a) Gross, Z.; Golubkov, G.; Simkhovich, L. *Angew. Chem., Int. Ed.* **2000**, *39*, 4045–4047. (b) Liu, H. Y.; Lai, T. S.; Yeung, L. L.; Chang, C. K. *Org. Lett.* **2003**, *5*, 617–620.
- (3) Reviews: (a) Goldberg, D. P. *Acc. Chem. Res.* **2007**, *40*, 626. (b) Abu-Omar, M. M. *Dalton Trans.* **2011**, *40*, 3435–3444.
- (4) Some major recent studies: (a) Kumar, A.; Goldberg, I.; Botoshansky, M.; Buchman, Y.; Gross, Z. *J. Am. Chem. Soc.* **2010**, *132*, 15233–15245. (b) Wang, S. H. L.; Mandimutsira, B. S.; Todd, R. C.; Ramdhanie, B.; Fox, J. P.; Goldberg, D. P. *J. Am. Chem. Soc.* **2004**, *126*, 18–19. (c) Umile, T. P.; Groves, J. T. *Angew. Chem., Int. Ed.* **2011**, *50*, 695–698.
- (5) Czernuszewicz, R. S.; Su, Y. O.; Stern, M. K.; Macor, K. A.; Kim, D.; Groves, J. T.; Spiro, T. G. *J. Am. Chem. Soc.* **1988**, *110*, 4158–4165.
- (6) (a) Groves, J. T. *J. Inorg. Biochem.* **2006**, *100*, 434–447. (b) Que, L. Jr. *Acc. Chem. Res.* **2007**, *40*, 493–500.
- (7) Collins, T. J.; Gordon-Wylie, S. W. *J. Am. Chem. Soc.* **1989**, *111*, 4511–4513.
- (8) (a) Mandimutsira, B. S.; Ramdhanie, B.; Todd, R. C.; Wang, H.; Zareba, A. A.; Czernuszewicz, R. S.; Goldberg, D. P. *J. Am. Chem. Soc.* **2002**, *124*, 15170–15171. (b) Lansky, D. E.; Mandimutsira, B.; Ramdhanie, B.; Clausen, M.; Penner-Hahn, J.; Zvyagin, S. A.; Telsler, J.; Krzystek, J.; Zhan, R.; Ou, Z.; Kadish, K. M.; Zakharov, L.; Rheingold, A. L.; Goldberg, D. P. *Inorg. Chem.* **2005**, *44*, 4485–4498.
- (9) (a) Cai, S.; Walker, F. A.; Licocchia, S. *Inorg. Chem.* **2000**, *39*, 3466–3478. (b) Ghosh, A.; Wondimagegn, T.; Parusel, A. B. *J. Am. Chem. Soc.* **2000**, *122*, 5100–5104. (c) Steene, E.; Wondimagegn, T.; Ghosh, A. *J. Phys. Chem. B* **2001**, *105*, 11406–11413; Addition/correction: *J. Phys. Chem. B* **2002**, *106*, 5312. (d) Zakhariyeva, O.; Schünemann, V.; Gerdan, M.; Licocchia, S.; Cai, S.; Walker, F. A.; Trautwein, A. X. *J. Am. Chem. Soc.* **2002**, *124*, 6636–6648. (e) Steene, E.; Dey, A.; Ghosh, A. *J. Am. Chem. Soc.* **2003**, *125*, 16300–16309. (f) Walker, F. A.; Licocchia, S.; Paolesse, R. *J. Inorg. Biochem.* **2006**, *100*, 810–837.
- (10) The difficulties of DFT with heme spin state energetics were recognized about a decade ago; the same studies showed that multiconfigurational perturbation theory provided a reasonable solution to a number of the problems: (a) Ghosh, A.; Gonzalez, E.; Vangberg, T.; Taylor, P. R. *J. Porphyrins Phthalocyanines* **2001**, *5*, 345–346. (b) Ghosh, A.; Persson, B. J.; Taylor, P. R. *J. Biol. Inorg. Chem.* **2003**, *8*, 507–511. (c) Ghosh, A.; Taylor, P. R. *Curr. Opin. Chem. Biol.* **2003**, *7*, 113–124.
- (11) Reviews on comparative performance of different exchange-correlation functionals in relation to transition metal complexes: (a) Harvey, J. N. *Struct. Bonding (Berlin)* **2004**, *112*, 151–183. (b) Ghosh, A. *J. Biol. Inorg. Chem.* **2006**, *11*, 712–724.
- (12) Selected recent studies on DFT calculations on transition metal spin state energetics: (a) Ghosh, A.; Gonzalez, E.; Tangen, E.; Roos, B. O. *J. Phys. Chem. A* **2008**, *112*, 12792–12798. (b) Swart, M. J. *Chem. Theory Comput.* **2008**, *4*, 2057–2066. (c) Takatani, T.; Sears, J. S.; Sherrill, C. D. *J. Phys. Chem. A* **2009**, *113*, 9231–9236. (d) Pierloot, K.; Vancoillie, S. *J. Chem. Phys.* **2008**, *128*, 034014.
- (13) For selected recent ab initio calculations on heme intermediates, see: (a) Vancoillie, S.; Zhao, H.; Radoń, M.; Pierloot, K. *J. Chem. Theory Comput.* **2010**, *6*, 576–582. (b) Chen, H.; Song, J.; Lai, W.; Wu, W.; Shaik, S. *J. Chem. Theory Comput.* **2010**, *6*, 940–953. (c) Chen, H.; Lai, W.; Shaik, S. *J. Phys. Chem. B* **2011**, *115*, 1727–1742. (d) Radoń, M.; Broclawik, E.; Pierloot, K. *J. Chem. Theory Comput.* **2011**, *7*, 898–908.
- (14) Ab initio calculations on metallocorroles: (a) Roos, B. O.; Veryazov, V.; Conradie, J.; Taylor, P. R.; Ghosh, A. *J. Phys. Chem.* **2008**, *112*, 14099–14102. (b) Pierloot, K.; Zhao, H.; Vancoillie, S. *Inorg. Chem.* **2010**, *49*, 10316–10329.
- (15) Ghosh, A.; Taylor, P. R. *J. Chem. Theory Comput.* **2005**, *1*, 597–600.
- (16) Ikezaki, A.; Takahashi, M.; Nakamura, M. *Dalton Trans.* **2011**, *40*, 9163–9168.
- (17) De Angelis, F.; Jin, N.; Car, R.; Groves, J. T. *Inorg. Chem.* **2006**, *45*, 4268–4276.
- (18) Becke, A. D. *Phys. Rev. A* **1988**, *38*, 3098–3100.
- (19) Perdew, J. P.; Wang, Y. *Phys. Rev.* **1986**, *B33*, 8822–8824. Erratum: Perdew, J. P. *Phys. Rev.* **1986**, *B34*, 7406.
- (20) Perdew, J. P.; Ernzerhof, M.; Burke, K. *J. Chem. Phys.* **1996**, *105*, 9982–9985.
- (21) Stephens, J.; Devlin, F. J.; Chabalowski, C. F.; Frisch, M. J. *J. Phys. Chem.* **1994**, *98*, 11623–11627.
- (22) Ahlrichs, R.; Kär, M.; Bäser, M.; Horn, H.; Hölmel, C. *Chem. Phys. Lett.* **1989**, *162*, 165–169.
- (23) The OLYP exchange-correlation functional is based on the OPTX exchange functional (Handy, N. C.; Cohen, A. *J. Mol. Phys.* **2001**, *99*, 403–412.) and the LYP correlation functional (Lee, C.; Yang, W.; Parr, R. G. *Phys. Rev.* **1988**, *B37*, 785–789).
- (24) Frisch, M. J.; Trucks, G. W.; Schlegel, H. B.; Scuseria, G. E.; Robb, M. A.; Cheeseman, J. R.; Scalmani, G.; Barone, V.; Mennucci, B.; Petersson, G. A.; Nakatsuji, H.; Caricato, M.; Li, X.; Hratchian, H. P.; Izmaylov, A. F.; Bloino, J.; Zheng, G.; Sonnenberg, J. L.; Hada, M.; Ehara, M.; Toyota, K.; Fukuda, R.; Hasegawa, J.; Ishida, M.; Nakajima, T.; Honda, Y.; Kitao, O.; Nakai, H.; Vreven, T.; Montgomery, Jr., J. A.; Peralta, J. E.; Ogliaro, F.; Bearpark, M.; Heyd, J. J.; Brothers, E.; Kudin, K. N.; Staroverov, V. N.; Kobayashi, R.; Normand, J.; Raghavachari, K.; Rendell, A.; Burant, J. C.; Iyengar, S. S.; Tomasi, J.; Cossi, M.; Rega, N.; Millam, N. J.; Klene, M.; Knox, J. E.; Cross, J. B.; Bakken, V.; Adamo, C.; Jaramillo, J.; Gomperts, R.; Stratmann, R. E.; Yazyev, O.; Austin, A. J.; Cammi, R.; Pomelli, C.; Ochterski, J. W.; Martin, R. L.; Morokuma, K.; Zakrzewski, V. G.; Voth, G. A.; Salvador, P.; Dannenberg, J. J.; Dapprich, S.; Daniels, A. D.; Farkas, Ö.; Foresman, J. B.; Ortiz, J. V.; Cioslowski, J.; Fox, D. J. *Gaussian 09*, Revision b01; Gaussian, Inc.: Wallingford, CT, 2009.
- (25) Weigend, F.; Ahlrichs, R. *Phys. Chem. Chem. Phys.* **2005**, *7*, 3297–3305.
- (26) Andersson, K.; Malmqvist, P.-Å.; Roos, B. O. *J. Chem. Phys.* **1991**, *96*, 1218–1226.
- (27) Malmqvist, P.-Å.; Pierloot, K.; Shahi, A. R. M.; Cramer, C. J.; Gagliardi, L. *J. Chem. Phys.* **2008**, *128*, 204109.
- (28) Aquilante, F.; De Vico, L.; Ferré, N.; Ghigo, G.; Malmqvist, P.-Å.; Neogrády, P.; Pedersen, T. B.; Pitőńák, M.; Reiher, M.; Roos, B. O.; Serrano-Andrés, L.; Urban, M.; Veryazov, V.; Lindh, R. *J. Comput. Chem.* **2010**, *31*, 224–247.
- (29) Reiher, M.; Wolf, A. *J. Chem. Phys.* **2004**, *121*, 10945–10956.
- (30) The standard IPEA-shifted zeroth order Hamiltonian for Second Order Perturbation Theory was used: Ghigo, G.; Roos, B.; Malmqvist, P.-Å. *Chem. Phys. Lett.* **2004**, *396*, 142–149.
- (31) The large ab initio calculations were facilitated by Cholesky decomposition (with a threshold of 10⁻⁶ au) of the two-electron repulsion integrals: Aquilante, F.; Malmqvist, P.-Å.; Pedersen, T. B.; Ghosh, A.; Roos, B. O. *J. Chem. Theory Comput.* **2008**, *4*, 694–702.
- (32) ANO-rcc basis sets are described in the following: (a) Roos, B. O.; Lindh, R.; Malmqvist, P.-Å.; Veryazov, V.; Widmark, P.-O. *J. Phys. Chem. A* **2004**, *108*, 2851–2858. (b) Roos, B. O.; Lindh, R.; Malmqvist, P.-Å.; Veryazov, V.; Widmark, P.-O. *J. Phys. Chem. A* **2005**, *109*, 6575–6579.
- (33) ANO-s basis sets are described in the following: Pierloot, K.; Dumez, B.; Widmark, P.-O.; Roos, B. *Theor. Chim. Acta* **1995**, *90*, 87–114.
- (34) Roos, B. O.; Andersson, K.; Fulscher, M.; Malmqvist, P.-Å.; Serrano-Andrés, L.; Pierloot, K.; Merchan, M. Multiconfigurational

perturbation theory: Applications in electronic spectroscopy. In *Advances in Chemical Physics: New Methods in Computational Quantum Mechanics*; Prigogine, I., Rice, S. A., Eds.; John Wiley & Sons: New York, 1996; Vol. 93, pp 219–331.

(35) Pierloot, K. Nondynamic Correlation Effects in Transition Metal Coordination Compounds. In *Computational Organometallic Chemistry*; Cundari, T. R., Ed.; Marcel Dekker, Inc.: New York, 2001.

(36) Pierloot, K. *Mol. Phys.* **2003**, *101*, 2083–2094.

(37) Radoń, M.; Broclawik, E.; Pierloot, K. *J. Chem. Theory Comput.* **2011**, *7*, 898–908.

(38) Vancoillie, S.; Zhao, H.; Tran, V. T.; Hendrickx, M. F. A.; Pierloot, K. *J. Chem. Theory Comput.* **2011**, *7*, 3961–3977.

(39) Unlike in ref 18, DFT methods appear to readily reproduce the observed singlet ground states of $Mn^V O$ corrolazines: Prokop, K. A.; de Visser, S. P.; Goldberg, D. P. *Angew. Chem., Int. Ed.* **2010**, *49*, 5091–5095.

(40) (a) Conradie, J.; Ghosh, A. *J. Phys. Chem. B* **2007**, *111*, 12621–12624. (b) Conradie, M. M.; Conradie, J.; Ghosh, A. *J. Inorg. Biochem.* **2011**, *105*, 84–91.

(41) Swart, M.; Ehlers, A. W.; Lammertsma, E. *Mol. Phys.* **2004**, *102*, 2467–2474.

(42) Swart, M.; Sola, F. M.; Bickelhaupt, F. M. *J. Chem. Phys.* **2009**, *131*, 094103.

(43) Noninnocence-induced saddling in Cu corroles: (a) Alemayehu, A. B.; Gonzalez, E.; Hansen, L.-K.; Ghosh, A. *Inorg. Chem.* **2009**, *48*, 7794–7799. (b) Alemayehu, A. B.; Hansen, L.-K.; Ghosh, A. *Inorg. Chem.* **2010**, *49*, 7608–7610. (c) Thomas, K.; Conradie, J.; Hansen, L.-K.; Ghosh, A. *Eur. J. Inorg. Chem.* **2011**, 1865–1870.

(44) (a) Bruckner, C.; Barta, C. A.; Brinas, R. P.; Bauer, J. A. K. *Inorg. Chem.* **2003**, *42*, 1673–1680. (b) Alemayehu, A.; Conradie, J.; Ghosh, A. *Eur. J. Inorg. Chem.* **2011**, 1857–1864.

(45) Alemayehu, A.; Ghosh, A. *J. Por. Phth.* **2011**, *15*, 106–110.

(46) Thomas, K. E.; Alemayehu, A. B.; Conradie, J.; Beavers, C. M.; Ghosh, A. *Inorg. Chem.* **2011**, *50*, 12844–12851.

(47) A unique $S = 1$ $Mn^V(NTs)$ corrole has been reported to carry out nitrene insertion into activated C–H bonds: Zdilla, M. J.; Abu-Omar, M. M. *J. Am. Chem. Soc.* **2006**, *128*, 16971–16979.